Environ Sci Pollut Res (2013) 20:6242–6255
DOI 10.1007/s11356-013-1672-3

RESEARCH ARTICLE

Removal and recovery of copper and nickel ions from aqueous solution by poly(methacrylamide-co-acrylic acid)/montmorillonite nanocomposites

Aboulfazl Barati · Mahdieh Asgari · Taghi Miri · Zohreh Eskandari

Received: 3 February 2013 / Accepted: 20 March 2013 / Published online: 16 April 2013

Abstract Nanocomposite hydrogels based on poly (methacrylamide-co-acrylic acid) and nano-sized montmorillonite were prepared by aqueous dispersion and in situ radical polymerization. Optimum sorption conditions were determined as a function of montmorillonite content, contact time, pH, and temperature. The equilibrium data of Cu^{2+} and Ni^{2+} conformed to the Freundlich and Langmuir isotherms in terms of relatively high regression values. The maximum monolayer adsorption capacity of the nanocomposite hydrogel (with 3 wt% montmorillonite content), as obtained from the Langmuir adsorption isotherm, was found to be 49.26 and 46.94 mg g^{-1} for Cu^{2+} and Ni^{2+}, respectively, at contact time=60 min, pH=6.8, adsorbent dose=100 mg/ml, and temperature=318 K. Kinetic studies of single system indicated that the pseudo-second order is the best fit with a high correlation coefficient (R^2=0.97–0.99). The result of five times sequential adsorption–desorption cycle shows a good degree of desorption and a high adsorption efficiency.

Keywords Nanocomposite · Hydrogel · Montmorillonite · Adsorption · Copper · Nickel

Introduction

Iran is in the top ten world metal producers in terms of copper production (Mollai et al. 2009). Demand for nickel and copper in the Iran market is progressively growing, while primary resources are being depleted. Nickel is used in combination with other metals to form alloys used for coins, jewelry, stainless steel, electroplating, to color ceramics, and in battery production (Schaumlöffel 2012). Copper, also, is used as a conductor of heat and electricity, a building material, and a constituent of various metal alloys and catalysts (Agrawal and Sahu 2010).

However, there are some health risks associated with these valuable metals. An increase in the intake of Cu^{2+} can cause health problems such as vomiting (Fukui et al. 1994), hypotension (López et al. 2004), melena (Oldenquist and Salem 1999), gastrointestinal distress (Knobeloch et al. 1994), and kidney failure (Kayaalt et al. 2010), while high Ni^{2+} intake can lead to nasopharynx (Metzgeroth et al. 2007), lung and dermatological diseases (Samitz and Katz 1975; Xu et al. 2011), birth effects (Brodziak-DopieraŁa et al. 2011), embolism (Szabó et al. 1985), and chronic bronchitis (Tessier and Pascal 2006). Therefore, it is essential to control the concentration of these heavy metals in the drinking water as well as, from the economical point of view, recover as much as possible of the copper and the nickel (Giannopoulou and Panias 2007).

To reduce heavy metal pollution problem and also recovery of these valuable metals, some traditional methods can be used including oxidation-reduction (Amara et al. 2008; Gupta et al. 2012; Saleh and Gupta 2012a, 2011; Saleh et al. 2011), filtration (Molinari et al. 2008), electrochemical treatment (Akbal and Camc 2011; Gupta et al. 2007a), solvent extraction (Ramachandra Reddy and Neela Priya 2005), reverse osmosis (Keane 1998), membrane separation (Pośpiech and Walkowiak 2007), and adsorption (Ghaee et al. 2012; Gupta et al. 2009, 2010, 2007b, 2011a, b, c; Saleh and Gupta 2012b). Because of high operation cost and low metal ion retention capacity of these methods, our low-cost adsorbents are an effective and economical method to adsorb and recover valuable Ni^{2+} and Cu^{2+} (Uğuzdoğan et al. 2010).

Responsible editor: Vinod Kumar Gupta

A. Barati (✉) · M. Asgari · T. Miri · Z. Eskandari
Chemical Engineering Department, Faculty of Engineering, Arak University, Arak 38156-8-8349, Iran
e-mail: a-barati@araku.ac.ir

Recently, the adsorption process with strong affinity and high loading capacity for targeted metal ions has developed much attention, which leads to modification of hydrogels (Demirbilek and Özdemir Dinç 2012). Hydrogels are loosely cross-linked hydrophilic polymers that can absorb, swell, and retain aqueous solution up to hundred times of their own weight (Barati et al. 2010). Some attempts have been made to modify the properties of hydrogels, for example, the incorporation of nano or micro particles of inorganic materials such as montmorillonite (Hua et al. 2010), kaolin (Pourjavadi et al. 2008), mica (Limparyoon et al. 2011), bentonite (Shirsath et al. 2011), laponite (Li et al. 2009), attapulgite (Zhang et al. 2007a, b), and zeolites (Bhardwaj et al. 2012) into polymer networks have been recently investigated.

Although many works have focused on the improvement of the swelling ability (Zhang et al. 2009), gel strength (Xu et al. 2010), mechanical and thermal stability (Zhang et al. 2007a, b) of composite hydrogel, only few literature have been focused on the adsorption and recovery capacity of heavy metal ions into the composite hydrogels (Yan et al. 2012; NüketTirtom et al. 2012; Hou et al. 2012).

Therefore, on the basis of our previous work on the preparation and ability to remove Pb^{2+} and Cd^{2+} by poly(acrylamide-co-acrylic acid) modified with porous materials (e.g., zeolites) (Zendehdel et al. 2011a), the adsorption capacity of the poly(methacrylamide-co-acrylic acid)/montmorillonite nanocomposites for Cu^{2+} and Ni^{2+} was studied in this paper. The effects of pH value and temperature of the Cu^{2+} and Ni^{2+} solutions, contact time with solution, montmorillonite content (weight percent), and the initial concentration of Cu^{2+} and Ni^{2+} solutions (C_i) were investigated. The adsorbed Cu^{2+} and Ni^{2+} ions can be desorbed from this adsorbent by a small amount of inorganic acid obtaining thus a high concentration solution of corresponding ions by which Ni^{2+} and Cu^{2+} can be enriched and recycled.

Material and methods

Chemicals

Methacrylamide (MAAm, Merck, Germany) was used as purchased. Acrylic acid (AA, Merck, Germany) was distilled under reduced pressure before use. Potassium hydroxide and *N*, *N*′-methylene bisacrylamide (Bis) were supplied by Merck, Germany. Ammonium persulfate (APS, analytical grade, Merck, Germany) was recrystallized from water. Natural montmorillonite (MMT) modified with a quaternary ammonium salt, dehydrogenated tallow dimethyl ammonium chloride (Cloisite® 15A with the average particle size of 75 nm measured by particle size analyzer) was supplied by Southern Clay Products Co., USA. Other agents were all analytical grade, and all solutions were prepared with distilled water.

Preparation of poly(MAAm-co-AA)/MMT nanocomposite hydrogels

The optimum molar ratio of initial materials for preparation of poly(MAAm-co-AA) considered at prior work in our laboratory (Zendehdel et al. 2010) but with small modifications. A series of poly(MAAm-co-AA)/MMT nanocomposite from MAAm, neutralized AA, and MMT was prepared using the one-step method via in situ intercalated polymerization (Zendehdel et al. 2011b). Typical preparation conditions for samples are as follows:

At first, potassium acrylate (KAA) was prepared by partially neutralizing a diluted acrylic acid solution with a predetermined amount of 50 wt% aqueous potassium hydroxide solution, which was added dropwise in an ice bath. Then, 10 g MAAm was dissolved in a mixing solution which consisted of 19 g of KAA, 2 g of Bis, and 55 ml of distilled water in a 250-ml four-neck flask equipped with a stirrer, a condenser, a thermometer, and a nitrogen line. Then, 0.62 g of MMT (ultrasound for 1 h before use for getting nano dispersed suspension) was slowly added to stirring monomer solution. The obtained suspension was mixed by a 300-rpm magnetic stirrer for 30 min. After removal of oxygen, this suspension was heated to 60 °C gradually, while 0.2 g of APS was introduced to initiate MAAm and KAA to generate macro-radicals. The temperature was kept at 70 °C for 3 h to complete the polymerization reaction. Then, the resulting product was washed several times with hydro ethanol solution and soaked in distilled water for 24 h. After that, the swelled hydrogels were taken out of the water and dried at 70 °C to a constant weight. The dried product was milled and screened. All samples used had a particle size in the range of 60–80 mesh.

Characterization

FTIR spectra of poly(MAAm-co-AA) hydrogel and poly (MAAm-co-AA)/MMT nanocomposite hydrogel were recorded (Perkin-Elmer, Spectrum 100) using KBr pellets. XRD patterns were obtained using a Philips X'Pert PRO Alpha-1diffractometer (Cu K radiation, λ=1.54056 A°, 40 kV, 40 mA) scanning from 5° to 80° at 4°/min. The morphology of the fractured specimens was observed on a XL30 SEM instrument (Philips Company, Netherlands) at an acceleration voltage of 30 kV after sputter coating with gold under vacuum.TGA was performed using a Perkin-Elmer (TGA 4000) Thermal Analyzer in air at a heating rate of 15 °C/min in the temperature range of 25–600 °C.

Adsorption experiment

Adsorption experiments were done in batch equilibrium mode. All experiments were done by mixing 100 ml of

aqueous solution of known concentration of Cu^{2+} and Ni^{2+} ions with 0.1 g of synthetic nanocomposites. The mixtures were shaken in an orbital shaker (THZ-98A) with 300 rpm at 298 K for a given contact time (5 to 180 min). The pH values of initial solutions were adjusted with 0.1 mol L^{-1} HCl or NaOH solutions by using a pH meter (Metrohm-744). The solution is filtered using a Whatman #40 filter paper. The filtrate was analyzed using inductively coupled

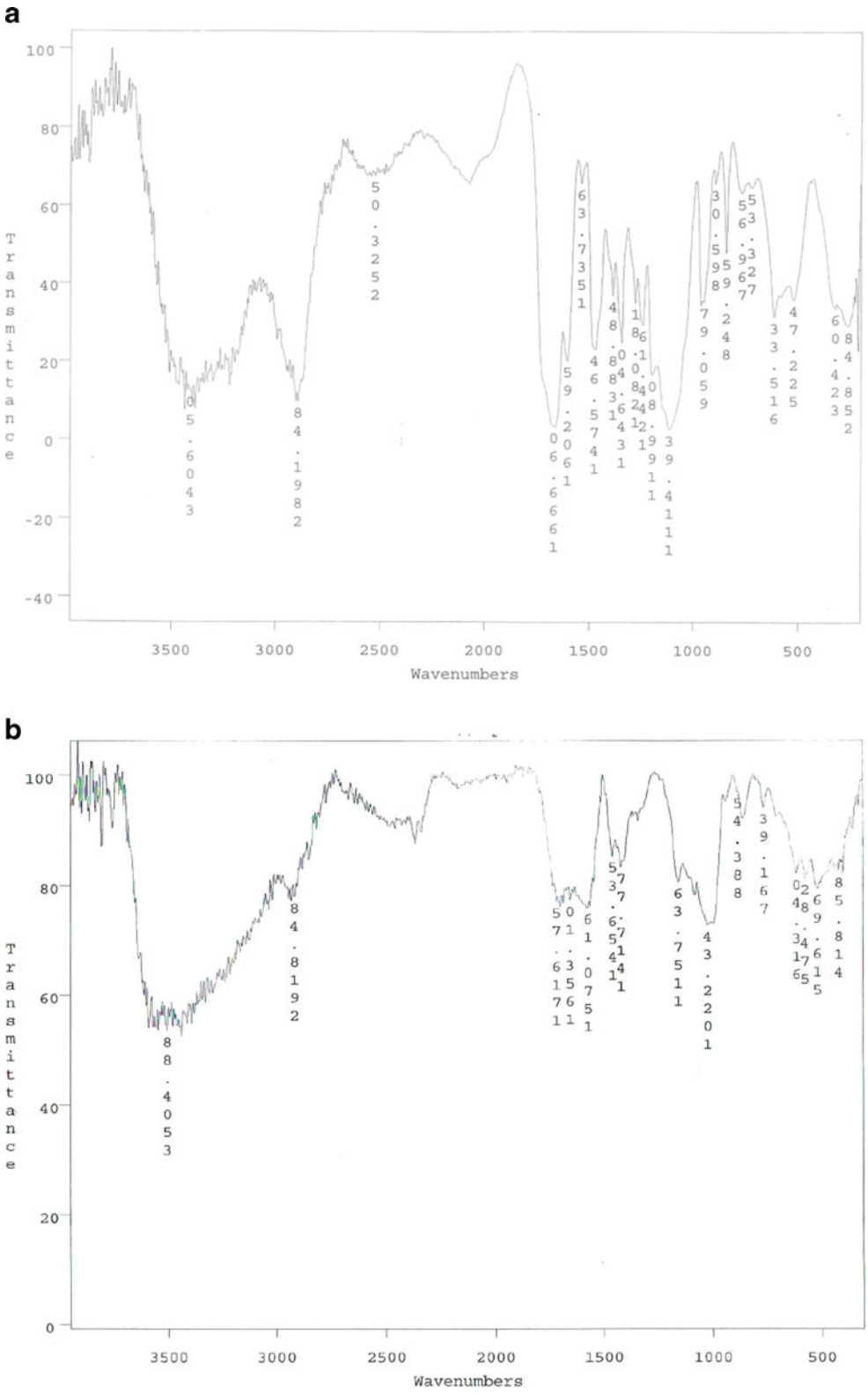

Fig. 1 FTIR spectra of **a** poly(MAAm-co-AA) and **b** poly(MAAm-co-AA)/MMT

plasma optical emission spectrometry Perkin Elmer Optima™ series using wavelength 324.75 and 231.60 nm for Cu^{2+} and Ni^{2+}, respectively (Futalan et al. 2011).

For adsorption studies, 25 up to 700 mg L^{-1} were chosen as the initial concentration of Cu^{2+} and Ni^{2+} single and binary solutions. The effects of pH were studied in the pH range of 2–11 at an initial concentration of 25 or 100 mg L^{-1} for both ions and contact time of 60 min. The adsorption capacity was calculated according to the following equation:

$$q_e = \frac{(C_i - C_e)V}{m} \quad (1)$$

Where q_e is the adsorption capacity, the amount of solute sorbed at equilibrium (milligrams per gram), C_i and C_e are the initial and final or equilibrium Cu^{2+} or Ni^{2+} concentration (milligrams per liter), m is the mass of adsorbent used, and V is the volume of Cu^{2+} or Ni^{2+} solution (milliliters). All the batch isotherm tests were replicated, and the experimental blanks were run in parallel. Check standards and blanks were run. Standard sources were used for instrument calibration and standard verification. All the experiments were done in triplicate, and average values are reported.

Desorption and regeneration

Desorption experiments were done in batch equilibrium mode by dispersing used (loaded) adsorbent (adsorbent dose in adsorption experiment=100 mg/ml; temperature=298 K; contact time=60 min; pH=6.8; MMT content=3 wt%) into two different volumes of 1 mol L^{-1} HCl solution (10 and 20 ml) and agitating at 298 K for 90 min in the orbital shaker. Then, the desorbed amount of Cu^{2+} and Ni^{2+} was obtained. In this study, we used 0.1 mol L^{-1} NaOH as the regenerating agent to investigate the regeneration ability of developing nanocomposite hydrogel adsorbent.

Enrichment and recovery

A 100-mg synthetic nanocomposite was contacted with 100 ml of Cu^{2+} or Ni^{2+} solution at 25 mg L^{-1} and agitated for 90 min at 25 °C to reach the equilibrium. Then, the used

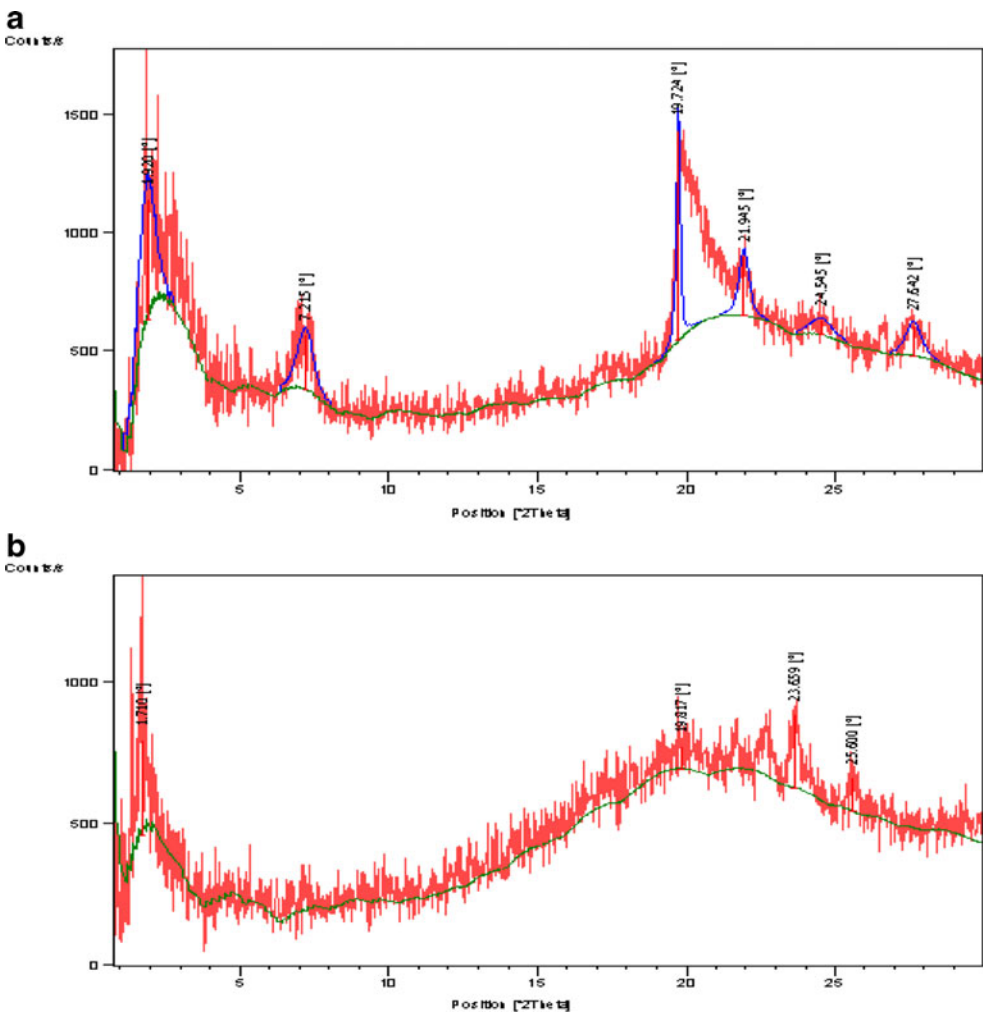

Fig. 2 X-ray diffraction patterns of **a** MMT and **b** poly(MAAm-co-AA)/MMT

adsorbent was separated using filtration and contacted again with another 100 ml of fresh solution at 25 mg L^{-1} to reach the adsorption equilibrium. A similar procedure was repeated until the percentage of adsorption A<95 % (Zheng et al. 2011). Using 1 mol L^{-1} HCl solution to elute and recover the Cu^{2+} or Ni^{2+} which retained on the adsorbent.

Results and discussion

FT-IR spectral analysis

The FT-IR spectra of poly(MAAm-co-AA) and poly(MAAm-co-AA)/montmorillonite nanocomposite hydrogel containing 3 wt% montmorillonite are shown in Fig. 1a and b, respectively. In Fig. 1a, a strong and broad absorption band has been observed at 3,406 cm^{-1} due to N-H groups of methacrylamide, and the peak at 1,666 cm^{-1} represents the carbonyl group. There is a shoulder at 1,715 cm^{-1} that corresponds to the carbonyl group of polyacrylate. Furthermore, one can see the two bonds at 1,388 and 1,537 cm^{-1} related to COO^- group in polyacrylate and the peaks at 1,475 and 2,891 cm^{-1} which represent the C-N and C-H bonding, respectively (Ni et al. 2005).

In (b) spectrum, the peaks of carbonyl shifted to around 1,653 cm^{-1} and the intensity of the peaks at 3,504 cm^{-1} corresponding to the reduced N-H and shifted to a lower frequency. This may be due to the formation of hydrogen bonding between COOH, NH_2 of the copolymer and hydroxyl group of Al-OH and Si-OH in montmorillonite. In addition, one can see two bands at about 1,022 cm^{-1} due to Si-O and 418 cm^{-1} related to Al-OH in the nanocomposite.

XRD analysis

The XRD patterns of montmorillonite and poly(MAAm-co-AA)/montmorillonite nanocomposite hydrogel are plotted in Fig. 2. The XRD pattern of montmorillonite shows a strong peak at $2\theta=2.39°$ which corresponds to a basal spacing of 30.1 A°. The absence of diffractions peaks for poly(MAAm-co-AA)/montmorillonite suggests that the clay layers have been exfoliated and dispersed in the polymer matrix to form a nanocomposite structure (Al et al. 2008; Liu et al. 2007). Hence, a broad peak observed at $2\theta=20°$ is due to poly(MAAm-co-AA) (Li et al. 2005).

SEM analysis

The micrographs of cross-linked poly(MAAm-co-AA) and poly(MAAm-co-AA)/montmorillonite nanocomposite containing 1 and 3 wt% of montmorillonite are depicted in Fig. 3a, b, and c, respectively. It is clearly observed that the poly(MAAm-co-AA) hydrogel shows a porous surface with interconnected pore, which interspersed on the surface. This surface morphology is beneficial for water intake, making the ions easily and quickly accessible to the reactive functional groups distributed within the polymeric networks. In (b) and (c) micrographs, it can be observed that the organo

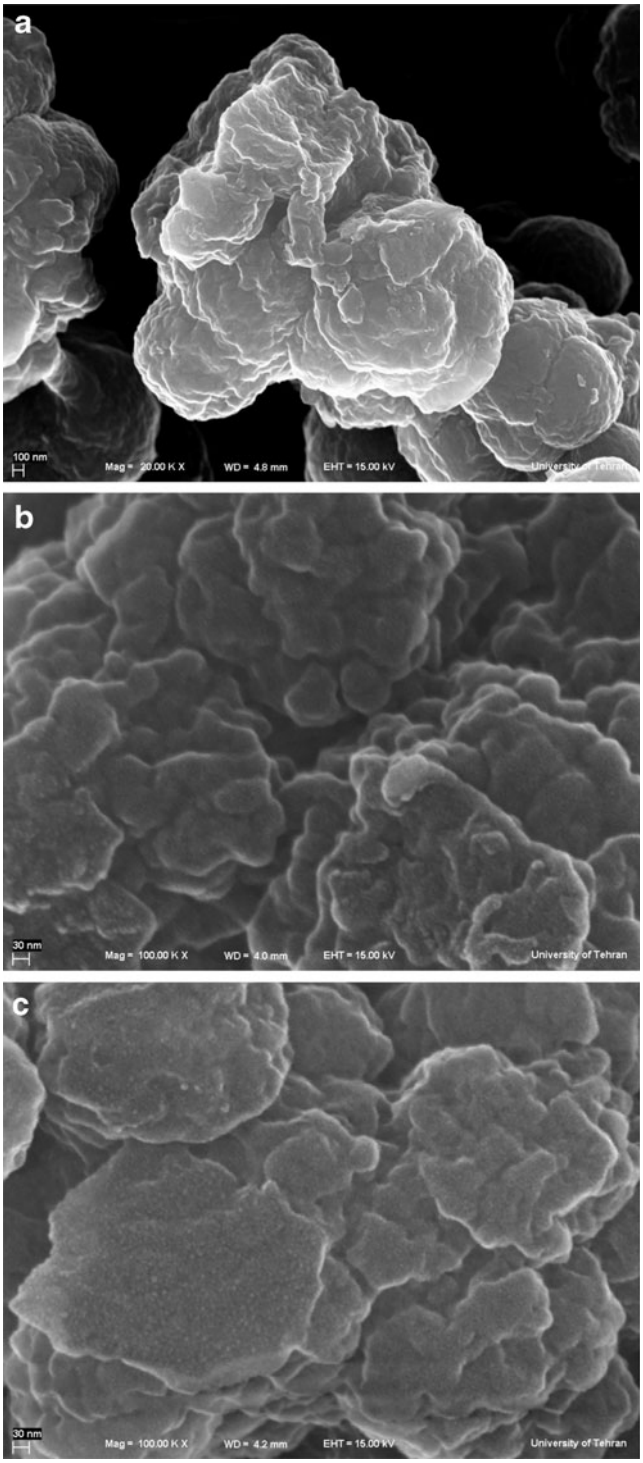

Fig. 3 Scanning electron micrographs of **a** cross section of poly(MAAm-co-AA) and surface of poly(MAAm-co-AA)/MMT **b** 1 wt% of MMT, **c** 3 wt% of MMT

montmorillonite nano particles are more finely dispersed in the polymer matrix.

Thermogravimetric analysis

The TGA of poly(MAAm-co-PA) hydrogel and poly (MAAm-co-PA)/montmorillonite nanocomposite hydrogel are shown in Fig. 4a and b, respectively. The initial decomposition temperature (T_{id}) was found to be 252 and 297 °C and the final decomposition temperature (T_{fd}) was observed as 609 and 615 °C for poly(MAAm-co-PA) hydrogel and poly(MAAm-co-PA)/montmorillonite nanocomposite hydrogel, respectively. The incorporation of montmorillonite in poly(MAAm-co-PA) matrix increased the thermal stability of the formulation, i.e., poly(MAAm-co-PA)/montmorillonite nanocomposite hydrogel. This can be attributed to the high

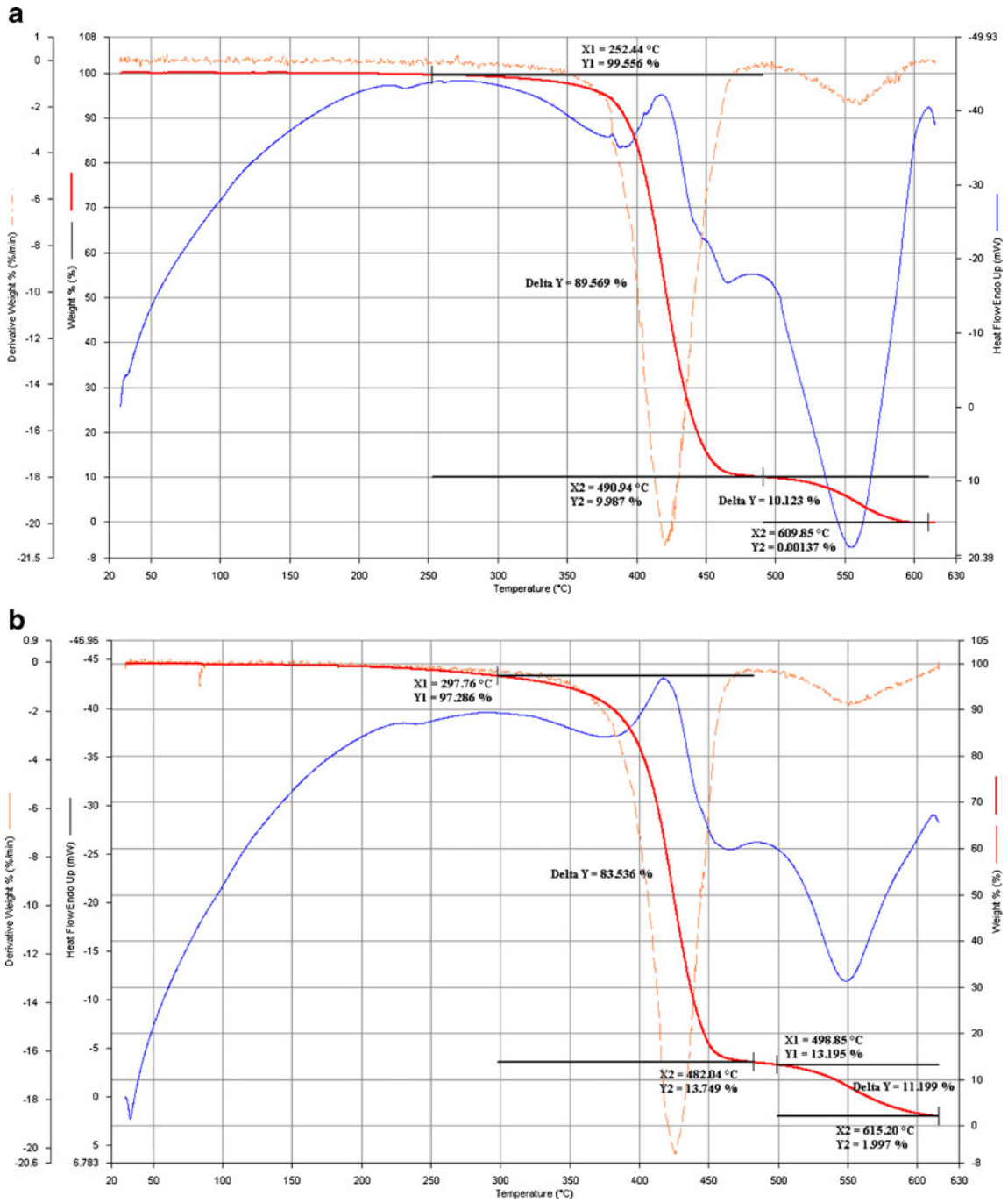

Fig. 4 TGA thermograms of **a** poly(MAAm-co-AA) and **b** poly(MAAm-co-AA)/MMT (3 wt% of MMT)

thermal stability of the clay minerals and to the interaction between the clay mineral particles and the polymer matrix (Li et al. 2005). Further, by comparison between Fig. 4a and b, it is observed that maximum loss in cross-linked polymer occurred after first stage of decomposition where temperature range was usually corresponded to the de-polymerization process. Since the proposed nanocomposite hydrogel is intended to be used for the recovery of Cu^{2+} and Ni^{2+} ions from the aqueous solution, and the removal process was normally carried out at room temperature, the nanocomposite polymer was totally stable in the room temperature, which varied between 27 and 32 °C.

Adsorption capacity

Figure 5 shows the effect of initial concentration of Cu^{2+} and Ni^{2+} ions on the adsorption capacity, respectively (pH=6.8, temperature=25 °C, contact time=60 min, and amount of MMT=3 wt%). Results show that the adsorption capacity increases with increasing the initial concentration of both ions up to 500 mg L^{-1}. This is attributed to the increase in Cu^{2+} or Ni^{2+} ion concentration resulting in an increase in the diffusion of ions into the polymeric network as a result of an increase in the driving force of the concentration gradient. However, by increasing the initial concentration of both ions from 500 to 700 mg L^{-1}, the amount of ions adsorbed remains nearly constant due to saturation of the adsorption sites at the adsorbents. However, even with very high initial concentration of 700 mg L^{-1} of Cu^{2+} and Ni^{2+} solutions, nanocomposite can adsorb about 29 mg g^{-1} of Cu^{2+} and 21 mg g^{-1} of Ni^{2+}.

The effect of contact time on the adsorption capacity was investigated at an initial Cu^{2+} or Ni^{2+} concentrations of 25 and 100 mg L^{-1} as shown in Fig. 6 (pH=6.8, temperature=25 °C, and amount of MMT=3 wt%). The adsorption increases with time up to 60 min for Cu^{2+} and up to 30 min for Ni^{2+} and then saturates. Thus, it appears that the adsorption is rapid, and the time to reach equilibrium is 60 min for Cu^{2+} and 30 min for Ni^{2+} ions. This rapid adsorption rate is consistent with the expected results derived from SEM analysis, which revealed their porous microstructure.

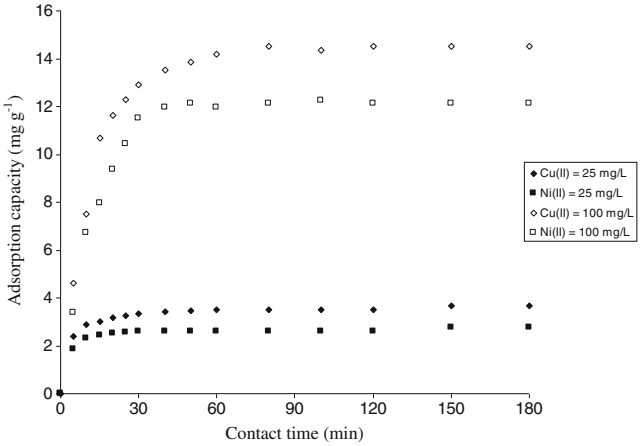

Fig. 6 Influences of contact time on the adsorption capacity of nanocomposite hydrogel for metal ions with different amount of C_i (pH=6.8; temperature=298 K; adsorbent dose=100 mg/100 ml; MMT content=3 wt%)

Figure 7 shows the adsorption capacity of Cu^{2+} and Ni^{2+} ions at different MMT levels in as-prepared nanocomposite hydrogel. The result shows that with increasing of MMT content from 1 to 3 wt% (C_i=100 mg L^{-1}, pH=6.8, temperature=25 °C, and contact time=60 min), the adsorption of Cu^{2+} and Ni^{2+} increased. According to the FT-IR analysis, Fig. 1b, –OH bond of MMT participated in the copolymerization and the formation of the exfoliated nanostructure in poly(MAAm-co-AA)/MMT, which may improve the polymeric network, and hence enhance the adsorption capacity. But any further increase in MMT content of nanocomposite

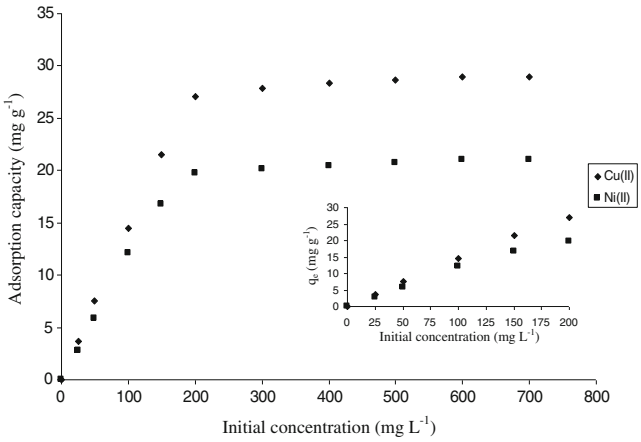

Fig. 5 Effect of Cu^{2+} and Ni^{2+} initial concentration on adsorption capacity of nanocomposite hydrogel (contact time=60 min; pH=6.8; temperature=298 K; adsorbent dose=100 mg/100 ml; MMT content=3 wt%)

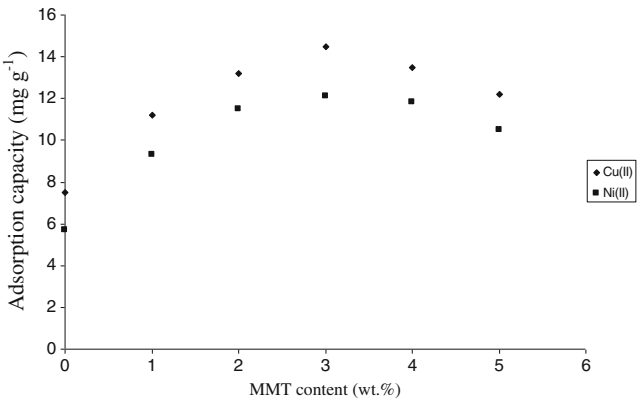

Fig. 7 Effect of MMT content on adsorption capacity of nanocomposite hydrogel (C_i=100 mg L^{-1}; pH=6.8; temperature=298 K; contact time=60 min, and adsorbent dose=100 mg/100 ml)

Table 1 Parameters of kinetic models of Cu^{2+} and Ni^{2+} adsorption onto nanocomposite hydrogel

Metal ions	C_i (mg L^{-1})	Pseudo-first order				Pseudo-second order			
		K_1 (min^{-1})	q_e^{exp}	q_e^{th}	R^2	K_2 (g mg^{-1} min^{-1})	q_e^{exp}	q_e^{th}	R^2
Cu^{2+}	25	0.0442	3.664	1.563	0.8446	0.0936	3.664	3.667	0.9999
	100	0.0617	14.500	11.806	0.9836	0.0060	14.500	16.58	0.9951
Ni^{2+}	25	0.0886	2.759	1.608	0.8885	0.1463	2.759	2.82	0.9997
	100	0.0919	12.100	14.005	0.9583	0.0028	12.100	18.31	0.9786

hydrogel had a reverse effect on the adsorption of both metal ions, and the adsorption capacity decreased. This is maybe because of –OH bond of hydrated montmorillonite, interaction between MMT with AA which became intensive. This means that more chemical and physical cross-link bonds were formed, and elasticity of polymer chains decreased. Consequently, the osmotic pressure between polymeric network and external solution for water permeation decreased which results in the lower adsorption capacity of poly(MAAm-co-AA)/MMT nanocomposite. This is in line with finding of Wang and co-worker who studied the adsorption performance of chitosan-g-poly(acrylic acid)/montmorillonite nanocomposite hydrogels for methylene blue (MB) and concluded a similar result that an appropriate MMT content was critical for improving the adsorption rate for MB (Wang et al. 2008).

Adsorption kinetics

The study of adsorption kinetics identifies what type of adsorption mechanism occurs. These models also describe the solute uptake rate, and evidently this rate controls the residence time of adsorbate uptake at the nanocomposite hydrogel–solution interface. To analyze Cu^{2+} and Ni^{2+} adsorption on the nanocomposite hydrogel, nonlinear form of pseudo-first-order (Langergren 1898) and pseudo-second-order (Ho et al. 1999) kinetic models was utilized and expressed as follows:

Pseudo-first-order model,

$$\log(q_e - q_t) = \log q_e - \frac{k_1 t}{2.303} \tag{2}$$

Pseudo-second-order model,

$$\frac{t}{q_t} = \frac{1}{k_2 q_e^2} + \frac{t}{q_e} \tag{3}$$

Where k_1 (grams per gram per minute) is the pseudo-first-order kinetic constant; k_2 (grams per milligram per minute) is the pseudo-second-order kinetic constant; q_e is the amount of solute sorbed at equilibrium (milligrams per gram), while q_t is the amount of solute sorbed at time t (milligrams per gram) before reaching equilibrium.

The conformity between experimental data and the model-predicted values was expressed by the correlation coefficients (R^2, values close or equal to 1). A relatively high R^2 value indicates that the model successfully describes the kinetics of Cu^{2+} and Ni^{2+} adsorption.

Table 1 shows the kinetic constants as well as the correlation coefficients, R^2 (C_i=25 and 100 mg L^{-1}, temperature= 298 K, pH=6.8, the amount of MMT=3 wt%). Pseudo-

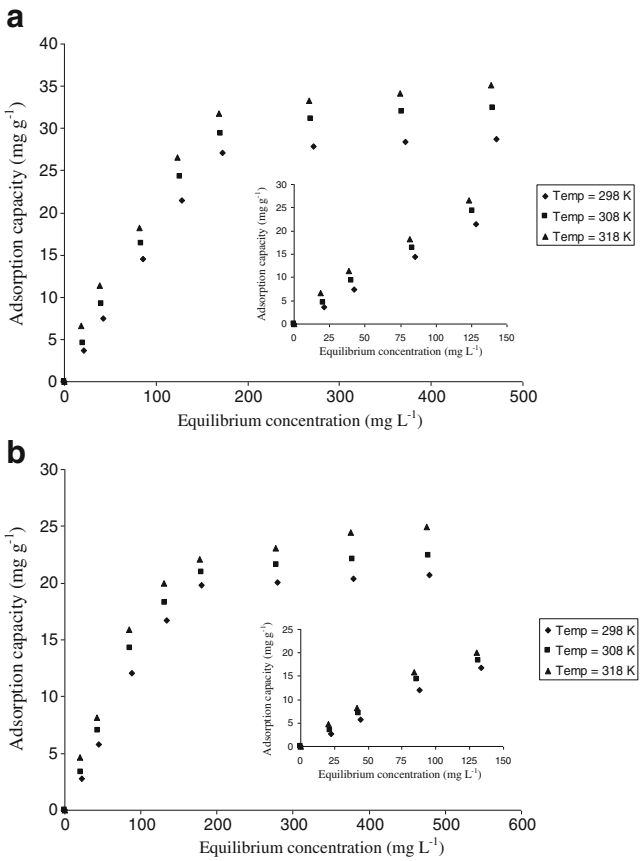

Fig. 8 Adsorption isotherms of **a** Cu^{2+} and **b** Ni^{2+} on nanocomposite hydrogel at different temperatures (contact time=60 min; pH=6.8; adsorbent dose=100 mg/100 ml; MMT content=3 wt%)

Table 2 Estimated adsorption isotherm parameters for Cu^{2+} and Ni^{2+} adsorption

Metal ions	Temperature (K)	Langmuir			Freundlich			Temkin		
		q_{max}	b	R^2	K_F	n	R^2	A_T	b_T	R^2
Cu^{2+}	298	588.23	2.95×10^{-4}	0.9995	0.1988	1.041	0.9988	0.0543	223.5	0.9498
	308	121.95	1.93×10^{-3}	0.9989	0.3433	1.144	0.9968	0.0619	220.4	0.9593
	318	49.26	8.23×10^{-3}	0.9941	0.8199	1.399	0.9977	0.0813	234.1	0.9495
Ni^{2+}	298	500.00	2.94×10^{-4}	0.9973	0.1489	1.042	0.9908	0.0541	297.6	0.9753
	308	208.33	7.66×10^{-4}	0.9956	0.2399	1.131	0.9968	0.0613	297.4	0.9876
	318	46.94	5.39×10^{-3}	0.9954	0.5097	1.338	0.9836	0.0759	311.5	0.9816

second-order equation has the highest correlation coefficient for both metal ions (R^2>0.98). Table 1 data indicate that the q_e^{th} values for the second-order model are closer to q_e^{exp} values (3.67 and 2.82 mg g^{-1} for the Cu^{2+} and Ni^{2+}, respectively) in comparison to first-order values. So, it can be concluded that Cu^{2+} and Ni^{2+} sorption onto the nanocomposite hydrogel seems to be more pseudo-second order, which means that chemisorption is the rate-controlling mechanism for adsorption of Cu^{2+} and Ni^{2+} onto our adsorbents.

Adsorption isotherms

Adsorption isotherm studies were carried out by fitting our data (see Fig. 8a, b) to the Langmuir, Freundlich, and Temkin isotherms. Adsorption isotherms describe how ions interact with adsorbent materials and therefore are critical in optimizing the use of adsorbents. The Langmuir isotherm is valid for monolayer sorption due to a surface of a finite number of identical sites and expressed in the linear form as Eq. 4.

$$\frac{1}{q_e} = \frac{1}{bq_{max}C_e} + \frac{1}{q_{max}} \tag{4}$$

Where q_e is the amount of adsorbed ions at equilibrium (millimoles per gram), q_{max} is the monolayer adsorption capacity of the adsorbent (millimoles per gram), C_e is the equilibrium concentration of ion solution (moles per liter), and b is the Langmuir adsorption constant (liters per mole) and is related to the free energy of adsorption. The Freundlich isotherm describes the heterogeneous surface energies by multilayer adsorption and is expressed in a linear form as Eq. 5.

$$\log q_e = \log K_F + \frac{1}{n}\log C_e \tag{5}$$

Where K_f includes adsorption extent (milligrams per gram), and n is an empirical parameter related to the intensity of adsorption, which varies with the nonlinearity between solution concentration and adsorption. The Temkin

Table 3 Comparison of Cu^{2+} and Ni^{2+} adsorption on poly(MMAm-co-AA)/MMT with other adsorbents

Metal ions	Adsorbents	Maximum adsorption capacity (mg g^{-1})	Equilibrium time (min)	Reference
Cu^{2+}	Natural zeolite	8.97	–	Erdan et al. 2004
	Acid-activated montmorillonite	32.30	200–300	Bhattacharyya and Gupta 2007
	Modified geothite	31.81	1,000–1,500	Li et al. 2007
	PVA-immobilized *Aspergillus niger*	34.13	20–30	Tsekova et al. 2009
	Chitosan-coated perlite beads	147.05	100–200	Swayampakula et al. 2009
	Poly (Methacrylamide-co-acrylic acid)/ montmorillonite	49.26	30	Present work
Ni^{2+}	Bentonite	4.32	–	Donat et al. 2005
	Sodium montmorillonite	10.65	230	Ijagbemi et al. 2010
	Clinoptilolite	15.55	500–1,000	Sprynskyy et al. 2006
	Chitosan	86.51	1,440	Paulino et al. 2007
	Chitosan-g-poly(acrylic acid)	161.8	30	Zheng et al. 2011
	O. hatei (untreated)	40.98	50–100	Gupta et al. 2010
	O. hatei (acid treated)	44.25	50–100	Gupta et al. 2010
	Poly (Methacrylamide-co-acrylic acid)/ montmorillonite	46.92	60	Present work

Table 4 Estimated adsorption isotherm parameters for Cu^{2+} and Ni^{2+} in (Cu-Ni) binary metal systems

Metal ions	Langmuir model			Freundlich model		
	q_{max}	b	R^2	K_F	n	R^2
Cu^{2+} (Cu-Ni)	64.52	2.815×10^{-3}	0.9876	0.1866	1.0364	0.9989
Ni^{2+} (Cu-Ni)	49.50	1.524×10^{-3}	0.9975	0.0668	0.9766	0.985

isotherm (Tempkin and Pyzhev 1940) is the early model describing the adsorption of metal ions onto adsorbents. The isotherm contains a factor that explicitly takes into account the adsorbent–adsorbate interaction and is based on the assumption that the free energy of sorption is a function of the surface coverage. The Temkin isotherm in the linear form is expressed as follows:

$$q_e = \frac{RT}{b_T}\ln A_T + \left(\frac{RT}{b_T}\right)\ln C_e \quad (6)$$

Where A_T is the equilibrium binding constant corresponding to the maximum binding energy (liters per milligram), b_T is the Temkin isotherm constant, T is the temperature (Kelvin) and R is the ideal gas constant (8.314 J mol^{-1} K^{-1}; Gupta et al. 2010)

The isotherm constants and correlation coefficient R^2 were calculated and summarized in Table 2. On comparing the linear regression values, it is concluded that the Langmuir and Freundlich isotherms are capable of representing the data more satisfactorily (R^2=0.98–0.99) than the Temkin isotherm (R^2=0.95–0.98). Both Cu^{2+} and Ni^{2+} have high correlation value (R^2>0.99) with Freundlich isotherm that the 1/n values were between 0 and 1 indicating the adsorption of $Cu^{2+}$and Ni^{2+} ions onto as-prepared nanocomposite was favorable at studied conditions. The extent of adsorption of Cu^{2+} and Ni^{2+} by different other adsorbent, collected from the literature, along with the results of the present study is included in Table 3. The data in the table indicate that synthesized nanocomposite hydrogel in current study has comparable adsorption capacity compared to many adsorbents.

Cu^{2+} may coexist with Ni^{2+} in industrial wastewater, and thus, investigation of the adsorption capacities of these coexisting ions in a binary system is important. For this binary system, the original Langmuir and Freundlich isotherm equations were applied to determine the effect of presence of another metal ion on the isotherm constants. In

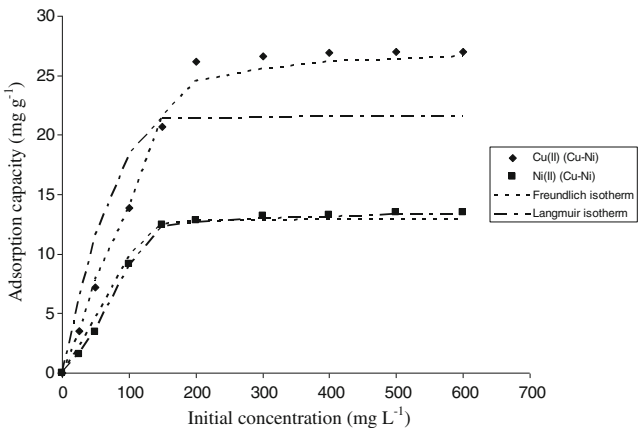

Fig. 9 Comparison of experimental isotherm data of binary systems of Cu-Ni against the theoretical non-linear plots generated using the Langmuir and Freundlich models (contact time=60 min; pH=6.8; temperature=298 K; adsorbent dose=100 mg/100 ml; MMT content=3 wt%)

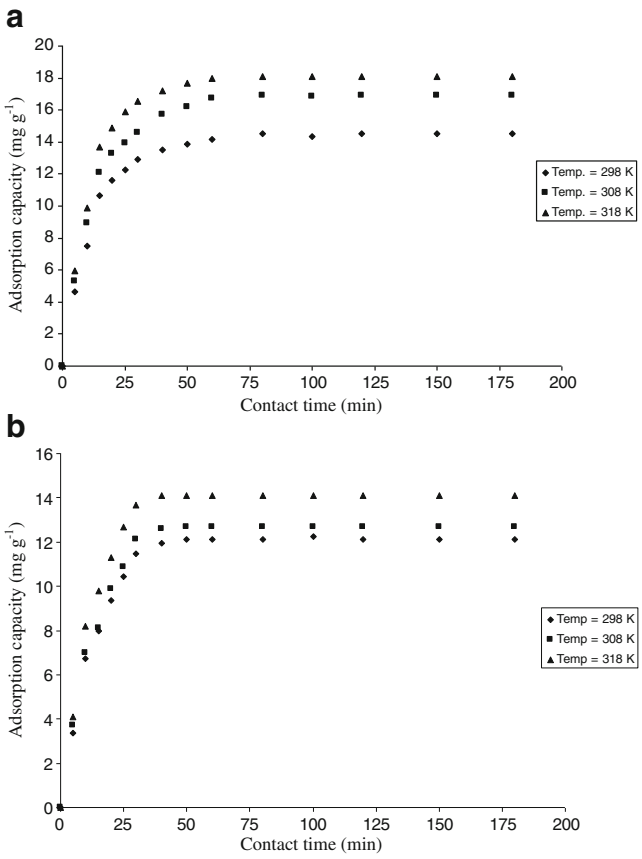

Fig. 10 Effect of temperature on the adsorption capacity of nanocomposite hydrogel for **a** Cu^{2+} and **b** Ni^{2+} (C_i=100 mg L^{-1}; pH=6.8; adsorbent dose=100 mg/100 ml; MMT content=3 wt%)

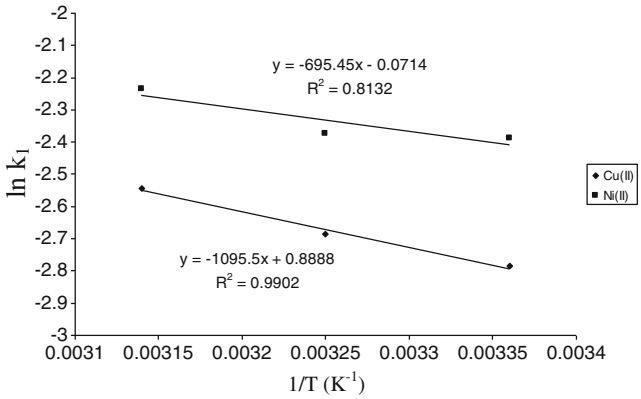

Fig. 11 Plot of pseudo-first order kinetic constant (ln k_1) vs. temperature ($1/T$). The activation energies of the adsorption process are determined from this graph

Table 4, the isotherm constant values for Cu-Ni system are reported. For Cu-Ni system, Cu^{2+} best fits Freundlich (R^2= 0.9989), while Ni^{2+} has a better correlation coefficient value for Langmuir (R^2=0.9975). Figure 9 shows the experimental data and models for binary system of Cu^{2+} and Ni^{2+}.

Effect of temperature on Cu^{2+} and Ni^{2+} adsorption

The adsorption behavior of nanocomposite hydrogel is affected by the temperature of the adsorption medium in many ways (C_i=100 mg L^{-1}, pH=6.8, and amount of MMT= 3 wt%). With increasing the temperature, the adsorption of heavy metal ions increased (Fig. 10a, b). The increase in the temperature of the adsorption medium is usually accompanied by the enhancement of the solution intake rate due to increased kinetic energy of solvent molecules. The activation energy of the solution intake process (swelling process) was determined by fitting the experimental data to the Arrhenius equation given below:

$$\ln k = ln(A) - \left(\frac{E_a}{RT}\right) \tag{7}$$

Where E_a (kilojoules per mole) is the apparent activation energy for the adsorption process, k the rate constant (minutes), A the Arrhenius constant, R the gas constant (8.314 J mol^{-1} K^{-1}), and T (Kelvin) is the solution temperature. The activation energies for the nanocomposite hydrogel, as determined from the slope of the linear plot (see Fig. 11) between the logarithm of k (the rate constant of pseudo-first-order kinetic equation (k_1; Table 5), were applied, and $1/T$ has been found to be 9.108 and 5.782 kJ mol^{-1} for Cu^{2+} and Ni^{2+}, respectively. It was obtained from this result that the adsorption involved physisorption and the process controlled by a diffusion process (Zou et al. 2006; Argun 2008).

Effect of pH on Cu^{2+} and Ni^{2+} adsorption

Figure 12 shows the effect of equilibrium pH on the amount of Cu^{2+} and Ni^{2+} adsorbed on as-prepared adsorbent (C_i=100 mg L^{-1}, temperature=298 K, pH=6.8, contact time=60 min, and amount of MMT=3 wt%). The adsorption capacity of both metal ions strongly depends on the solution pH. It can be seen from Fig. 12 that the adsorption capacity increased from 2.3 to 14.5 mg g^{-1} when pH of solution media increased from 2.1 to 6.8, but further increment of pH from 6.8 to 11.5 decreased the adsorption capacity of both metal ions. This is because when the pH of the medium is low (pH=2), the carboxylic groups of poly(potassium acrylate) are almost in an undissociated state and, therefore, these polymeric chains are closely packed through hydrogen bonding. When pH of the adsorbing medium increases from pH=2, the carboxylic groups dissociate into COO^- and result in relaxation of the networks by breaking the hydrogen bonds. Also, in this situation, more mobile ions (K^+ ions) exist in the hydrogel which may make the ion-exchange reaction between Cu^{2+} or Ni^{2+} ions and exchangeable cations existing in the composite happen very easily. This in turn increases the diffusion of water molecules into the network, thereby increasing the adsorbing capacity. When the pH of the

Table 5 Parameters of kinetic models of Cu^{2+} and Ni^{2+} adsorption onto nanocomposite hydrogel in different solution temperature

Metal ions	Temperature (K)	Pseudo-first order				Pseudo-second order			
		K_1 (min^{-1})	q_e^{exp}	q_e^{th}	R^2	K_2 (g mg^{-1} min^{-1})	q_e^{exp}	q_e^{th}	R^2
Cu^{2+}	298	0.0617	14.500	11.806	0.9836	0.0060	14.500	16.580	0.9951
	308	0.0682	16.900	15.991	0.9849	0.0042	16.900	20.208	0.9955
	318	0.0785	18.100	17.065	0.9889	0.0045	18.100	21.462	0.9926
Ni^{2+}	298	0.0919	12.100	14.005	0.9583	0.0028	12.100	18.313	0.9786
	308	0.0931	12.700	14.930	0.9453	0.0022	12.700	20.792	0.9792
	318	0.1071	14.100	17.412	0.9511	0.0019	14.100	23.698	0.9711

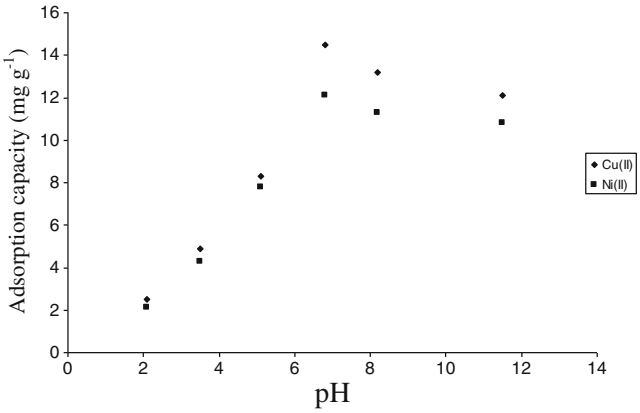

Fig. 12 Effects of pH on adsorption capacity of nanocomposite hydrogel for Cu^{+2} and Ni^{+2} (contact time=60 min; temperature=298 K; adsorbent dose=100 mg/100 ml; MMT content=3 wt%)

adsorbing medium is greater than 7, where the number of carboxylate anions reaches the maximum level, no more repulsion could be expected in the cross-linked hydrogel. This causes expulsion of water molecules from within the hydrogel into the media due to the weakening of the hydrogen bonds formed between water molecules and cross-linked hydrogel chains. The formation of $Cu(OH)_2$ or $Ni(OH)_2$ precipitation is another cause of the decrease in adsorbing capacity when the pH value of adsorbing medium is in the alkaline range (Zheng et al. 2010).

Desorption and regeneration study

Desorption studies are necessary for optimization of the regeneration of the nanocomposite, so that it can be used again to adsorb metal ions as well as for the recovery process of the Cu^{2+} and Ni^{2+} ions from the saturated nanocomposite hydrogel According to Wang et al. (2009), for desorption of Cu^{2+} and Ni^{2+}, the best performance was obtained using 1 mol L^{-1} HCl solution with desorption ratios of 96 and 98 %, respectively.

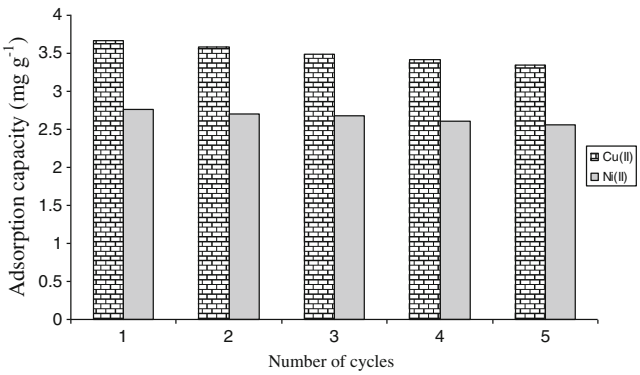

Fig. 13 Regeneration studies of poly(MAAm-co-AA)/MMT after five cycles

Reusing ability of an adsorbent by a regeneration process is an important parameter. To test the reusability of the adsorbent, adsorption–desorption cycles were repeated five times using the same adsorbent. Figure 13 shows the adsorption capacities of the adsorbents for Cu^{2+} and Ni^{2+} ions over five successive adsorption–desorption cycles. The results show that the adsorption capacity of the adsorbents slightly decreased with an increase in adsorption–desorption cycles. As shown in Fig. 13, more than 90 and 92 % of the initial adsorption capacities were obtained after fifth cycle of desorption for Cu^{2+} and Ni^{2+} ions, respectively. Therefore, poly (MAAm-co-AA)/MMT nanocomposite hydrogel is a good reusable adsorbent and could be successfully utilized for the recovery of heavy metal ions from water and wastewater.

Conclusion

Poly(methacrylamide-co-acrylic acid)/montmorillonite nanocomposite hydrogel was synthesized, characterized, and was used for the adsorption of Cu^{2+} and Ni^{2+} from aqueous solution. The as-prepared adsorbent not only possesses good chemical stability but also shows good affinity to Cu^{2+} and Ni^{2+} ions, with the maximum adsorption capacity of 29 and 21 mg g^{-1}, respectively. Some important factors affecting the adsorption such as contact time, initial metal concentration, temperature, and pH were studied. The equilibrium data of Cu^{2+} were best fitted the Freundlich isotherm, while those of Ni^{2+} followed the Langmuir isotherm. The kinetic data indicated that the adsorption kinetics followed the pseudo-second-order kinetic model. The high adsorption capacity and average desorption efficiency during the consecutive five-time adsorption–desorption processes of poly (MAAm-co-AA)/MMT nanocomposites implied that the nanocomposites possess the potential of regeneration and reuse. From the results above, it could be concluded that poly(MAAm-co-AA)/MMT nanocomposite hydrogel is an quite effective adsorbent for the removal and recovery of Cu^{2+} and Ni^{2+} from aqueous solution.

In summary, the proposed method is technically effective. How to prepare the nanocomposite hydrogel adsorbent and how to operate it optimally based on the effect of operation conditions on the adsorption process have been discussed. Furthermore, the proposed method is economically effective as well. The suggested adsorbent is relatively cheap to make and also provides a better chance of recovering the heavy metals adsorbed.

Acknowledgments The authors thank the Arak University Research Fund for providing financial support of this work.

References

Agrawal A, Sahu KK (2010) Problems, prospects and current trends of copper recycling in India: an overview. Res Conserv Rec 54:401–416

Akbal F, Camc S (2011) Copper, chromium and nickel removal from metal plating waste water by electrocoagulation. Desalination 269:214–222

Al E, Güçlü G, İyim TB, Emik S, Özgümüş S (2008) Synthesis and properties of starch-graft-acrylic acid/Na-montmorillonite superabsorbent nanocomposite hydrogels. J Appl Polym Sci 109:16–22

Amara M, Kerdjoudj H, Bouguelia A, Trari M (2008) A combination between membrane selectivity and photoelectrochemistry to the separation of copper, zinc and nickel in aqueous solutions. J Membrane Sci 312:125–131

Argun ME (2008) Use of clinoptilolite for the removal of nickel ions from water: kinetics and thermodynamics. J Hazard Mater 150:587–595

Barati A, Norouzi H, Sharafoddinzadeh S, Davarnejad R (2010) Swelling kinetics modeling of cationic methacrylamide-based hydrogels. World Appl Sci J 11:1336–1341

Bhardwaj D, Sharma M, Sharma P, Tomar R (2012) Synthesis and surfactant modification of clinoptilolite and montmorillonite for the removal of nitrate and preparation of slow release nitrogen fertilizer. J Hazard Mater 227–228:292–300

Bhattacharyya KG, Sen Gupta S (2007) Adsorptive accumulation of Cd(II), Co(II), Cu(II), Pb(II) and Ni(II) from water on montmorillonite: influence of acid activation. J Colloid Interf Sci 310:411–424

Brodziak-DopieraŁa B, Kwapuliński J, Sobczyk K, Kowol J (2011) The occurrence of nickel and other elements in tissues of the hip joint. Ecotox Environ Safe 74:630–635

Demirbilek C, Özdemir Dinç C (2012) Synthesis of diethylaminoethyl dextran hydrogel and its heavy metal ion adsorption characteristics. Carbohyd Polym 90:1159–1167

Donat R, Akdogan A, Erdem E, Cetisli H (2005) Thermodynamics of Pb^{2+} and Ni^{2+} adsorption onto natural bentonite from aqueous solutions. J Colloid Interf Sci 286:43–52

Erdem E, Karapinar N, Donat R (2004) The removal of heavy metal cations by natural zeolites. J Colloid Interf Sci 280:309–314

Fukui H, Yamamoto M, Sasaki S, Sato S (1994) Possible involvement of peripheral 5-HT_4 receptors in copper sulfate-induced vomiting in dogs. Eur J Pharmacol 257:47–52

Futalan CM, Kan C, Dalida ML, Hsien K, Pascua C, Wan M (2011) Comparative and competitive adsorption of copper, lead and nickel using chitosan immobilized on bentonite. Carbohyd Polym 83:528–536

Ghaee A, Shariaty-Niassar M, Barzin J, Zarghan A (2012) Adsorption of copper and nickel ions on macroporous chitosan membrane: equilibrium study. Appl Surf Sci 258:7732–7743

Giannopoulou I, Panias D (2007) Copper and nickel recovery from acidic polymetallic aqueous solutions. Miner Eng 20:753–760

Gupta VK, Ali I, Saini VK (2007a) Defluoridation of wastewaters using waste carbon slurry. Water Res 41:3307–3316

Gupta VK, Jain R, Varshney S (2007b) Electrochemical removal of the hazardous dye Reactofix Red 3 BFN from industrial effluents. J Colloid Interf Sci 312:292–296

Gupta VK, Mittal A, Malviya A, Mittal J (2009) Adsorption of carmoisine A from wastewater using waste materials—bottom ash and deoiled soya. J Colloid Interf Sci 335:24–33

Gupta VK, Rastogi A, Nayak A (2010) Biosorption of nickel onto treated alga (*Oedogonium hatei*): application of isotherm and kinetic models. J Colloid Interf Sci 342:533–539

Gupta VK, Agarwal S, Saleh T (2011a) Synthesis and characterization of alumina-coated carbon nanotubes and their application for lead removal. J Hazard Mater 185:17–23

Gupta VK, Agarwal S, Saleh T (2011b) Chromium removal by combining the magnetic properties of iron oxide with adsorption properties of carbon nanotubes. Water Res 45:2207–2212

Gupta VK, Gupta B, Rastogi A, Agarwal S, Nayak A (2011c) A comparative investigation on adsorption performances of mesoporous activated carbon prepared from waste rubber tire and activated carbon for a hazardous azo dye-Acid Blue 113. J Hazard Mater 186:891–901

Gupta VK, Ali I, Saleh T, Nayak A, Agarwal S (2012) Chemical treatment technologies for waste-water recycling—an overview. RSC Adv 2:6380–6388

Ho YS, McKay G (1999) Pseudo-second order model for sorption process. Process Biochem 34:451–465

Hou H, Zhou R, Wu P, Wu L (2012) Removal of Congo red dye from aqueous solution with hydroxyapatite/chitosan composite. Chem Eng J 211–212:336–342

Hua S, Yang H, Wang W, Wang A (2010) Controlled release of ofloxacin from chitosan–montmorillonite hydrogel. Appl Clay Sci 50:112–117

Ijagbemi CO, Baek MH, Kim DS (2010) Montmorillonite surface properties and sorption characteristics for heavy metal removal from aqueous solutions. J Hazard Mater 174:746–755

Kayaalt Z, Mergen G, Söylemezoğlu T (2010) Effect of metallothionein core promoter region polymorphism on cadmium, zinc and copper levels in autopsy kidney tissues from a Turkish population. Toxicol Appl Pharm 245:252–255

Keane MA (1998) The removal of copper and nickel from aqueous solution using Y zeolite ion exchangers. Colloid Surfaces A: Physicochem Eng Aspects 138:11–20

Knobeloch L, Ziarnik M, Howard J, Theis B, Farmer D, Anderson H, Proctor M (1994) Gastrointestinal upsets associated with ingestion of copper-contaminated water. Environ Health Persp 102:958–961

Langergren S (1898) Zur theorie der sogenannten adsorption geloster stoffe, Kungliga Svenska Vetenskapsakademines. Handlingar 24:1–39

Li A, Liu RF, Wang AQ (2005) Preparation of starch-graft-poly(acrylamide)/attapulgite superabsorbent composite. J Appl Polym Sci 98:1351–1357

Li P, Kim NH, Hui D, Rhee KY, Lee JH (2009) Improved mechanical and swelling behavior of the composite hydrogels prepared by ionic monomer and acid-activated Laponite. Appl Clay Sci 46:414–417

Li W, Zhang S, Shan X (2007) Surface modification of goethite by phosphate for enhancement of Cu and Cd adsorption. Colliods Surf A 293:13–19

Limparyoon N, Seetapan N, Kiatkamjornwong S (2011) Acrylamide/2-acrylamido-2-methylpropane sulfonic acid and associated sodium salt superabsorbent copolymer nanocomposites with mica as fire retardants. Polym Degrad Stabil 96:1054–1063

Liu PS, Li L, Zhou NL, Zheng J, Wei SH, Shen J (2007) Waste polystyrene foam-graft-acrylic acid/montmorillonite superabsorbent nanocomposite. J Appl Polym Sci 104:2341–2349

López F, Martínez-Lage JF, Hernández-Palazón J, López R, Alarcón E (2004) Actividad de la cobre-zinc superóxido dismutasa en un modelo de lesión cerebral isquémica global sin hipotensión arterial. Neurocirugía 15:151–158 (in Spanish)

Metzgeroth G, Back W, Schultheis B, Maywald O, Kuhn C, Hehlmann R, Hastka J (2007) Intestinal-type adenocarcinoma situated in the nasopharynx. Cytopathology 18:59–63

Molinari R, Poerio T, Argurio P (2008) Selective separation of copper (II) and nickel (II) from aqueous media using the complexation–ultrafiltration process. Chemosphere 70:341–348

Mollai H, Sharma R, Pe-Piper G (2009) Copper mineralization around the Ahar batholith, north of Ahar (NW Iran): evidence for fluid evolution and the origin of the skarn ore deposit. Ore Geol Rev 35:401–414

Ni Y, Ge X, Zhang Z (2005) Preparation and characterization of ZnS/poly(AAm-co-AAc) dendritically nanocomposites by γ-irradiation. Mater Sci Eng 119:51–54

Nüket Tirtom V, Dinçer A, Becerik S, Aydemir T, Çelik A (2012) Comparative adsorption of Ni(II) and Cd(II) ions on epichlorohydrin crosslinked chitosan–clay composite beads in aqueous solution. Chem Eng J 197:379–386

Oldenquist G, Salem M (1999) Parental copper sulfate poisoning causing acute renal failure. Nephrol Dial Transpl 14:441–443

Paulino AT, Guilherme MR, Reis AV, Tambourgi EB, Nozaki J, Muniz EC (2007) Capacity of adsorption of Pb2+ and Ni2+ from aqueous solutions by chitosan produced from silkworm chrysalides in different degrees of deacetylation. J Hazard Mater 147:139–147

Pośpiech B, Walkowiak W (2007) Separation of copper(II), cobalt(II) and nickel(II) from chloride solutions by polymer inclusion membranes. Sep Purif Technol 57:461–465

Pourjavadi A, Ayyari M, Amini-Fazl MS (2008) Taguchi optimized synthesis of collagen-g-poly(acrylic acid)/kaolin composite superabsorbent hydrogel. Eur Polym J 44:1209–1216

Ramachandra Reddy B, Neela Priya D (2005) Process development for the separation of copper(II), nickel(II) and zinc(II) from sulphate solutions by solvent extraction using LIX 84 I. Sep Purif Technol 45:163–167

Saleh T, Gupta VK (2011) Fictionalization of tungsten oxide into MWCNT and its application for sunlight-induced degradation of rhodamine B. J Colloid Interf Sci 362:337–344

Saleh T, Agarwal S, Gupta VK (2011) Synthesis of MWCNT/MnO_2 and their application for simultaneous oxidation of arsenite and sorption of arsenate. Appl Catal B-Environ 106:46–53

Saleh T, Gupta VK (2012a) Photo catalyzed degradation of hazardous dye methyl orange by use of a composite catalyst consisting of multi-walled carbon nanotubes and titanium dioxide. J Colloid Interf Sci 371:101–106

Saleh T, Gupta VK (2012b) Column with CNT/magnesium oxide composite for lead (II) removal from water. Environ Sci Pollut Res 19:1224–1228

Samitz MH, Katz SA (1975) Nickel dermatitis hazards from prostheses. Brit J Dermatol 92:287–290

Schaumlöffel D (2012) Nickel species: analysis and toxic effects. J Trace Elem Med Bio 26:1–6

Shirsath SR, Hage AP, Zhou M, Sonawane SH, Ashokkumar M (2011) Ultrasound assisted preparation of nanoclay Bentonite–FeCo nanocomposite hybrid hydrogel: a potential responsive sorbent for removal of organic pollutant from water. Desalination 281:429–437

Sprynskyy M, Buszewski B, Terzyk AP, Namiesnik J (2006) The study of selection mechanism of heavy metals (Pb, Cu, Ni and Cd) on clinoptilolite. J Colloid Interf Sci 304:21–28

Swayampakula K, Boddu VM, Nadavala SK, Abburi K (2009) Competitive adsorption of Cu(II), Co(II) and Ni(II) from their binary and tertiary aqueous solutions using chitosan-coated perlite beads as biosorbent. J Hazard Mater 170:680–689

Szabó K, Balogh I, Gergely A (1985) Endogenous nickel release in injured patients: a possible cause of myocardial damage. Injury 16:613–620

Tempkin MI, Pyzhev V (1940) Kinetics of ammonia synthesis on promoted iron catalyst. Acta Phys Chim USSR 12:327–356

Tessier DM, Pascal LE (2006) Activation of MAP kinases by hexavalent chromium, manganese and nickel in human lung epithelial cells. Toxicol Lett 167:114–121

Tsekova K, Todorova D, Dencheva V, Ganeva S (2009) Biosorption of copper (II) and cadmium (II) from aqueous solutions by free and immobilized biomass of *Aspergillus niger*. Bioresour Technol 101:1727–1731

Uğuzdoğan E, Baki DE, Sermet Kabasakal O (2010) The use of polyethyleneglycolmethacrylate-co-vinylimidazole (PEGMA-co-VI) microspheres for the removal of nickel(II) and chromium(VI) ions. J Hazard Mater 177:119–125

Wang L, Zhang J, Wang A (2008) Removal of methylene blue from aqueous solution using chitosan-g-poly(acrylic acid)/montmorillonite superadsorbent nanocomposite. Colloid Surface A: Physicochem Eng Aspects 322:47–53

Wang X, Zheng Y, Wang A (2009) Fast removal of copper ions from aqueous solution by chitosan-g-poly(acrylic acid)/attapulgite composites. J Hazard Mater 168:970–977

Xu K, Tan Y, Chen Q, An H, Li W, Dong L, Wang P (2010) A novel multi-responsive polyampholyte composite hydrogel with excellent mechanical strength and rapid shrinking rate. J Colloid Interf Sci 345:360–368

Xu Z, Ren T, Xiao C, Li H, Wu T (2011) Nickel promotes the invasive potential of human lung cancer cells via TLR4/MyD88 signaling. Toxicology 285:25–30

Yan H, Yang L, Yang Z, Yang H, Li A, Cheng R (2012) Preparation of chitosan/poly(acrylic acid) magnetic composite microspheres and applications in the removal of copper(II) ions from aqueous solutions. J Hazard Mater 229–230:371–380

Zendehdel M, Barati A, Alikhani H (2010) Synthesis and characterization of poly (AAm-co-AAc)/NaA nanocomposite and removal of methylene blue with it. J Iran Chem Res 3:161–165

Zendehdel M, Barati A, Alikhani H (2011a) Removal of heavy metals from aqueous solution by poly(acrylamide-co-acrylic acid) modified with porous materials. Polym Bull 67:343–360

Zendehdel M, Kalateh Z, Alikhani H (2011b) Efficiency evaluation of NaY zeolite and TiO_2/NaY zeolite in removal of methylene blue dye from aqueous solutions. Iran J Environ Health Sci Eng 8:265–273

Zhang D, Wang D, Duan J, Ge S (2009) Research on the long time swelling properties of poly (vinyl alcohol)/hydroxyapatite composite hydrogel. J Bionic Eng 6:22–28

Zhang J, Wang Q, Wang A (2007) Synthesis and characterization of chitosan-*g*-poly(acrylic acid)/attapulgite superabsorbent composites. Carbohyd Polym 68:367–374

Zheng Y, Hua S, Wang A (2010) Adsorption behavior of Cu^{+2} from aqueous solution onto starch-g-poly(acrylic acid)/sodium humate hydrogels. Desalination 263:170–175

Zheng Y, Huang D, Wang A (2011) Chitosan-g-poly(acrylic acid) hydrogel with crosslink polymeric networks for Ni^{2+} recovery. Anal Chim Acta 687:193–200

Zou W, Han R, Chen Z, Jinghua Z, Shi J (2006) Kinetic study of adsorption of Cu(II) and Pb(II) from aqueous solutions using manganese oxide coated zeolite in batch mode. Colloid Surface A: Physicochem Eng Aspects 279:238–246